Bioelectromagnetics 23:230–238 (2002)
DOI 10.1002/bem.10010

Increased Mouse Survival, Tumor Growth Inhibition and Decreased Immunoreactive p53 After Exposure to Magnetic Fields

Santi Tofani,[1]* Marcella Cintorino,[2] Domenico Barone,[3] Michele Berardelli,[1] Maria Margherita De Santi,[2] Adriana Ferrara,[1] Renzo Orlassino,[1] Piero Ossola,[1] Katia Rolfo,[1] Flavio Ronchetto,[1] Sergio Antonio Tripodi,[2] and Piero Tosi[2]

[1]Ivrea Hospital ASL n. 9, Ivrea (TO), Italy
[2]University of Siena, Institute of Pathological Anatomy and Histology, Siena, Italy
[3]LCG-RBM BIOSCIENCE Spa, Biomedical Research Institute "A. Marxer," Colleretto Giacosa, Italy

The possibility that magnetic fields (MF) cause antitumor activity in vivo has been investigated. Two different experiments have been carried out on nude mice bearing a subcutaneous human colon adenocarcinoma (WiDr). In the first experiment, significant increase in survival time (31%) was obtained in mice exposed daily to 70 min modulated MF (static with a superimposition of 50 Hz) having a time average total intensity of 5.5 mT. In the second independent experiment, when mice bearing tumors were exposed to the same treatment for four consecutive weeks, significant inhibition of tumor growth (40%) was reported, together with a decrement in tumor cell mitotic index and proliferative activity. A significant increase in apoptosis was found in tumors of treated animals, together with a reduction in immunoreactive p53 expression. Gross pathology at necroscopy, hematoclinical/hematological and histological examination did not show any adverse or abnormal effects. Since pharmacological rescue of mutant p53 conformation has been recently demonstrated, the authors suggest that MF exposure may obtain a similar effect by acting on redox chemistry connected to metal ions which control p53 folding and its DNA-binding activity. These findings support further investigation aimed at the potential use of magnetic fields as anti-cancer agents. Bioelectromagnetics 23:230–238, 2002.

Key words: apoptosis; colon carcinoma (WiDr) xenograft; nude mice

INTRODUCTION

The biological effects linked to the possible carcinogenesis induced by low intensity magnetic fields (MF), such as those that may be found in the environment and the underlying mechanisms, are being widely debated. Data from scientific literature are controversial. Experimental studies indicate that environmental MF are unlikely to be cancer initiators, and further investigations are needed to clarify potential factors acting together with MF to eventually promote cancer onset [Koifman, 1993; Hendee and Boteler, 1994]. Some epidemiological data support an association between surrogate measurement of MF and an increased risk of childhood leukemia, even though the body of evidence is weak to demonstrate that exposure to extremely low frequency (ELF) MF is a human cancer health hazard [NRC, 1996; NIEHS, 1999].

In contrast, the use of higher (by 1000 times) MF intensity has allowed proven therapeutic effects on bone disorders, particularly in bone fractures [Basset et al., 1982]. More recently, several studies seem to indicate a possibly wider medical role for MF. Among them, some reported the induction of apoptosis in human leukemic cells [Hisamitsu et al., 1997], while others demonstrated micronucleus formation and apoptosis induced by ELF–EMF on a human squamous carcinoma cell line (SCL II), but not in a human amniotic fluid cell line (AFC) [Simko et al., 1998]. Other studies indicate an effect of EMF on the tyrosine kinase-dependent phospholipase Cγ2 activation in DT40 lymphoma B cells [Dibirdik et al., 1998; Kristupaitis et al., 1998].

The possibility that MF may contribute to cancer research and therapy has recently been investigated.

*Correspondence to: Dr. Santi Tofani, Department of Medical Physics, Ivrea Hospital, Via di Vittorio 1, 10015 Ivrea (TO), Italy. E-mail: fisicasan@asl.ivrea.to.it

Received for review 31 January 2001; Final revision received 23 July 2001

MF of more than 1 mT have been hypothesized to exert anticancer activity [Tofani, 1999]. A mechanism for this activity is the possible MF influence on free radical recombination processes that activate p53 gene dependent survival mechanisms. ELF MF of 100 mT were used to inhibit tumor growth in mice [de Seze et al., 2000]. Static MF of 110 mT were used to enhance chemotherapy in mice [Gray et al., 2000]. A combination of static and ELF MF with average intensity ranging from 2.48 to 5.5 mT was used to study their influence on apoptosis in tumor growth in nude mice [Tofani et al., 2001].

In our previous studies we selected the MF characteristics (frequency, intensity and modulation) that affect tumor cell response in vitro in terms of apoptosis-like death induction and in vivo in terms of tumor growth inhibition in nude mice bearing WiDr human colon adenocarcinoma cells. The MF exposure conditions that gave the best results in the above tumor growth study are used in the present study, where we show that MF exposure significantly increased the survival of nude mice bearing the WiDr cells. The tumor growth inhibition was associated with the loss of p53 and an increase in apoptosis, together with a decrement in tumor cell mitotic index and proliferative activity. These effects were associated with the absence of adverse responses such as morphological changes in normal renewing (i.e., bone marrow), slowly proliferating (i.e., hepatocytes) and static (i.e., neurons) cells.

MATERIALS AND METHODS

Animal Selection and Housing

Nude female mice (CD-1, nu-nu), 5 weeks old, were purchased from Charles River Italia (Calco, Lecco, Italy). The fitness of mice was assessed during the acclimatization period (1 week) on the basis of physical examination and on verification of their body weight (24 ± 2 g).

Animals were housed in air conditioned rooms at a temperature of $26 \pm 2\,^{\circ}$C, with 40–60% humidity, 10–15 filtered air changes per hour, and artificial lighting with a circadian cycle of 12 h. Each cage, sterilized and protected with a filter top, contained three nude mice. Cages were changed once a week under a laminar flow hood. A γ-irradiated diet (4 RF21, Mucedola, Settimo Milanese, Milano, Italy) and drinking water, sterilized by autoclaving, were available ad libitum to all the animals. Use and care of animals in this experiment was in accord with Directive 86/609/EEC, enforced by the Italian D.L. No. 116 of January 27, 1992 and approved by the Official RBM Veterinarian.

Cell Culture and Animal Inoculation

WiDr (ATCC CCL-218) human colon adenocarcinoma cells were harvested by trypsinization and the number of viable cells was determined by trypan blue exclusion test. The cells were washed once with serum-free medium and resuspended in the same medium to a final density of $10^7 \pm 5\%$ cells/0.2 ml. On day of the experiment, animals were given an s.c. interscapular cell injection with a sterile 1 ml tuberculin syringe fitted with a 21 gage needle (0.2 ml/mouse of the cell suspension kept in melting ice under continuous agitation).

Treatment Protocols and MF Characteristics

The MFs were generated by a pair of coils mounted horizontally with their axes lying in the same plane and orthogonally to the ground. The coils were connected with a circuit providing D.C. and A.C. current at 50 Hz. The A.C. current was obtained from the 50 Hz line, using a two voltage variable transformer, and the D.C. current was obtained with a bridge. A 100 Hz ELF MF component had an intensity of about 3% of the static magnetic field (SMF). The harmonic content of the A.C. field was 2%. During the exposure, each mouse, exposed and sham exposed, was held in an individual plexiglas box (14.7 cm $\times$ 3.6 cm $\times$ 3.6 cm) placed between the two coils. Mouse box temperature was periodically checked by means of a Luxtron mod. 1000B electromagnetic compatible fiber optic thermometer and proved to be within the room temperature oscillation. MF exposure was characterized and continuously monitored during each treatment.

The MF exposure parameters were selected in a previous study as those that gave the best results in the growth inhibition study [Tofani et al., 2001]. The exposure was made, using modulated MF, static with a superimposition of ELF at 50 Hz, whose field intensity characteristics are reported in Table 1 and Figure 1 in terms of field intensity and wave form characteristics,

TABLE 1. The MF Characteristics for the Treatment (rms Intensity Values)

Time (min)	5	5	5	20	5	5	5	20
Static MF (mT)	3.0	4.0	3.0	4.0	3.0	4.0	3.0	4.0
ELF (mT)	1.5	2.5	1.5	2.5	1.0	1.5	1.0	1.5

The field uniformity (percentage standard deviation considering nine measurement points) throughout the mouse box is about $\pm 10\%$.

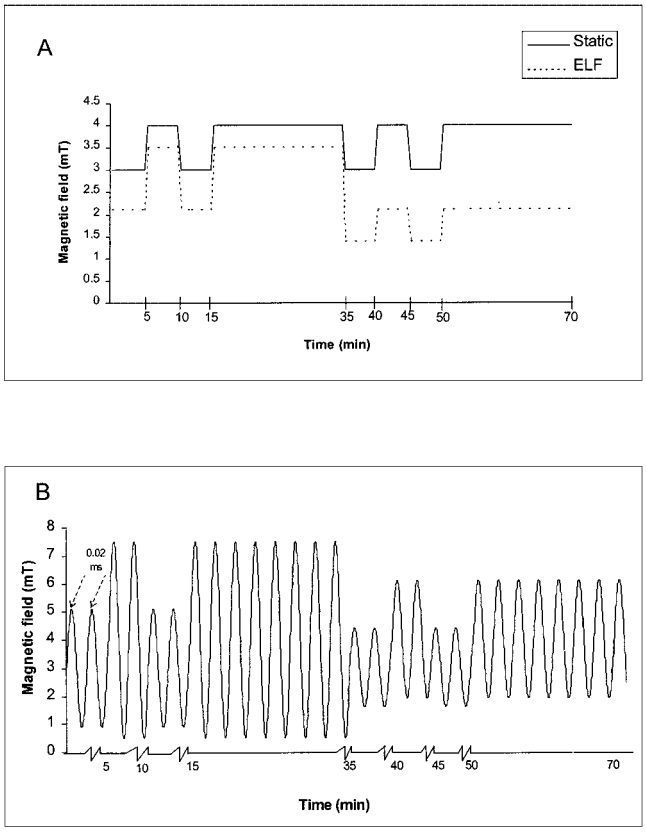

Fig. 1. **A:** Diagram of the MF exposure condition during the 70 min treatment (ELF MF are peak values). **B:** MF waveform characteristics of the eight different steps forming the MF treatment.

respectively. The time averaged total intensity of this treatment is 5.5 mT. The animals were exposed for 70 min, once a day, 5 days a week, for the entire survival time in the animal survival study and for four consecutive weeks in the case of the tumor growth inhibition study.

The sham exposed animals were handled and treated in the same conditions, that is, held in the exposure box, experiencing also the same temperature and humidity, for the same time as exposed animals, but with the exposure apparatus power off.

Animal Survival Study

Animals were inoculated with WiDr cells at day 0, randomized and exposed to treatment every working day (5 days/week) from day 1 up to death. Thirty-three animals were used, 16 treated and 17 sham treated with MF. Mice were allowed to live up to their natural death or were sacrificed with an overdose of pentobarbital if found in severe clinical condition, in order to avoid undue suffering. The presence of tumor was confirmed in all animals. The survival index was evaluated as the ratio between the cumulative survival time of the treated animals and that of the sham treated ones. This index was evaluated by summing, for each experimental group, the survival times of treated mice and dividing it by the sum of the survival times of the sham treated mice multiplied by 100.

Tumor Growth Study

This study was carried out on 21 mice, 12 MF treated and 9 sham treated. Fifteen days after tumor cell inoculation, the animals were randomly assigned to the two experimental groups, and treatment began on the same day. Six additional mice (controls), used as reference for tumor growth, were housed throughout the experiment without any manipulation.

The tumor nodule size was measured in two dimensions with an autoclaved caliper at the beginning of treatment (V_b) and extracted at the autopsy (V_e). The volume of the mass was calculated in mm^3 according to the following formula:

$$\text{Volume} = \frac{(\text{greatest diameter}) \times (\text{smallest diameter})^2}{2}$$

The tumor growth inhibition was determined as the ratio between the difference of the average extracted volume (V_e), calculated considering all sham and treated mice, and the average extracted volume (V_e) of sham mice $\times$ 100.

At the end of the study, 24 h after the 20th treatment, the mice were killed under deep pentobarbital anesthesia (0.2 ml/mouse of a 5% solution i.p.) by bleeding from the ventral aorta. The animals were subjected to autopsy at which time the tumor mass/es were dissected from the implantation site, the skin removed and the actual tumor masses weighed. Parts of the tumor masses were appropriately fixed for histopathology, immunohistochemistry, and transmission electron microscopy (TEM) investigation. In addition, different organs (brain, heart, kidneys, liver, lungs, axillary, inguinal and mediastinal lymphnodes, ovaries, skin from the tumoral mass sites, spleen and bone marrow from the femur) were also taken at autopsy from each listed animal and fixed for safety assessment and toxicological evaluation of treatment.

Histopathology. Specimens from the experimental tumors (21 cases from the tumor growth study) were fixed in 10% buffered neutral formalin and embedded in paraffin blocks. Sections (4 ± 0.5 μm) were collected on electrostatically charged slides (Super-Frost Plus, Bio-optica). Necrosis, fibrosis and inflammatory reaction were detected at light microscopy on Hematoxylin–Eosin stained sections. These modifications were blind scored by two independent observers ($+ \rightarrow +++$) according to semiquantitative criteria.

Mitoses were also evaluated and the mitotic index (MI) was reported by measuring their total number in at least 10 noncontiguous, randomly selected high power fields (HPF), avoiding necrotic areas, up to a total number of 5,000 cells.

Immunohistochemistry. Immunohistochemical staining to evaluate Mib1 and p53 expression was performed using the APAAP method on formalin fixed, paraffin embedded tissues. After drying, dewaxing, and rehydration, the sections were washed in distilled water. For antigen retrieval, slides were then processed in a microwave oven in cytrate buffer pH 6 (750 W for 5 min, 3 cycles). After washing in distilled water for 10 min, they were preincubated with normal rabbit serum (DAKO, Copenhagen, Denmark) for 20 min, and diluted 1:10 in Tris buffered saline pH 7.6 (TBS) to prevent nonspecific binding. After removing serum by blotting, the slides were incubated overnight at 4 °C with primary antibodies: Mib1, 1:100 Immunotech (Marseille, France) and p53 1:40 DBA (DBA, Segrate, Italy), then washed in TBS for 5 min. All the antibodies were diluted in TBS. The sections were successively incubated with the secondary antibody (rabbit-antimouse immunoglobulins—DAKO Z259) diluted 1:30 in TBS and finally with APAAP (DAKO D651) diluted 1:50 in TBS. Each incubation was performed for 30 min at room temperature and followed by three washes with TBS. The second and the third stages of the procedure were repeated for 10 min to amplify the immunostaining. The alkaline phosphatase was revealed by naphtol and new fuchsin as substrate. The endogen phosphatase was blocked by adding 1 mM levamisole to the substrate solution. The sections were then washed for 5 min with running tap water, weakly counterstained with Mayer's Hematoxylin and mounted with aqueous mountant (Aquatex, Merck, Germany). Both Mib1 and p53 were considered positive when nuclei showed a fuchsia red stain.

Negative controls were obtained for each antibody by replacing the specific mAb with a class-matched irrelevant antibody or TBS.

The number of positive and negative nuclei was calculated in 10 randomly selected HPF (avoiding necrotic areas), using an eyepiece grid and a 40× objective. A labeling index (LI) for Mib1 and p53 was calculated as follows:

$$\mathrm{LI} = \frac{\text{number of labeled cells}}{\text{total number of examined cells}} \times 100$$

The intraobserver variation coefficient was 2.9%.

Nucleic Acid Hybridization. In each case, one section of tumor mass was employed to evaluate the in situ apoptosis with the TUNEL method using a commercial kit (Apotech, Diatech, Italy), with two modifications: proteinase was substituted by microwave incubation and the revelation system (streptavidin) by the avidin-biotin system. Diaminobenzidine was used as substrate.

The apoptotic index (AI) for each animal was scored by evaluating the total number of apoptotic cells on 5,000 cells/mouse in at least 10 noncontiguous randomly selected (avoiding necrotic areas) HPF (40×). The intraobserver variation coefficient was 3.0%.

Transmission Electron Microscopy. The specimens for TEM were fixed in 2.5% glutaraldehyde buffered with 0.1M Na–cacodylate for 3 h at 4 °C, washed in the same buffer, post fixed in osmium tetroxyde, dehydrated in increasing concentrations of acetone and embedded in Araldite. Semithin sections were stained with Toluidin blue. Ultrathin sections from significant areas were counterstained with Uranyle acetate and Pb citrate and observed in a Zeiss EM109 transmission electron microscope.

Safety and Toxicology Assessment

Organs and tissues. Each organ was fixed, embedded in paraffin, sectioned and stained as described in the histopathology paragraph. In doubtful cases, i.e., axillary/inguinal lymphnodes and other tissues selected for tumoral metastases, further sections were prepared and examined.

Blood. Whole blood, collected from the ventral aorta of mice sacrified 24 h after the 20th treatment, under deep pentobarbital anesthesia, was analyzed for alkaline phosphate (kinetic-colorimetric method on serum at 37 °C. A-Gent alkaline phosphatase test, Abbott Lab. Diagn. Div.); total bilirubin (colorimetric method on serum. A-Gent bilirubin test, Abbott Lab. Diagn. Div.); calcium (colorimetric method on serum. A-Gent calcium test, Abbott Lab. Diagn. Div.); creatinine (kinetic-colorimetric method on serum, creatinine test, Abbott Lab. Diagn. Div.); phosphorus (UV method on serum, phosphorus test, Abbott Lab. Diagn. Div.); urea nitrogen (enzymatic method on serum. Urea-UV test, Abbott Lab. Diagn. Div.); uric acid (enzymatic-colorimetric method. Peridochrom Uric Acid, Boehringer Mannheim GmbH-Diagn.); alanine aminotransferase (kinetic method on serum at 37 °C. ALT test, Abbott Lab. Diagn. Div.); aspartate aminotransferase (kinetic method on serum at 37 °C. AST test, Abbott Lab. Diagn. Div.); γ glutamyltransferase (kinetic-colorimetric method. Monotest, Boehringer Mannheim GmbH-Diagn.); leukocyte, erythrocyte,

mean corpuscular volume (MCV), platelet count (PLT) and mean platelet volume (MPV) (using the "Cellanalyzer 480" cell counter Delcon); hemoglobin (colorimetric method, using the "Cellanalyzer 480" cell counter Delcon); hematocrit {calculated with the following formula: hematocrit = MCV × number of erythrocytes}; mean corpuscular hemoglobin (MCH) {calculated with the following formula: MCH = [hemoglobin (g/100 ml × 10)]/[herythrocytes ($\times 10^6$/mm^3)]}; mean corpuscular hemoglobin concentration (MCHC) {calculated with the following formula: MCHC = [hemoglobin (g/100 ml × 100)]/[hematocrit)]}.

Statistical Analysis

Means and SDs were calculated for all data sets. Each animal was considered as an experimental unit. For these experiments, a variance homogeneity F test was used followed by comparison using the Student's test in case of variance homogeneity or otherwise by the Wilcoxon test. Data referring to survival time of sham-treated and treated mice were compared using the Mantell-Cox test. A P value of < 0.05 was considered statistically significant.

All the biological and pathological exams carried out were blind. All the animals were coded and the persons in charge of the MF treatment were not involved in the biological and pathological exams at any levels.

RESULTS

Animal Survival Study

Figure 2 reports the curves of the survival time from the beginning of treatment versus the percentage of living treated and sham treated animals. All the mice died with a tumor in the subcutaneous site. After approximately 4 months of the MF exposure, the two survival curves, which up to that time had been superimposed, began to diverge and, after 6 months, on the death of the last sham-treated mouse (around day 195) treated group showed a survival time which gradually became significantly higher than the sham one. The survival index for this treatment was 131%, i.e., 31% of survival time increase. At the end of the experiment (day 310), two MF treated mice, both bearing tumors, were still alive and were sacrificed even though only one was in a critical condition.

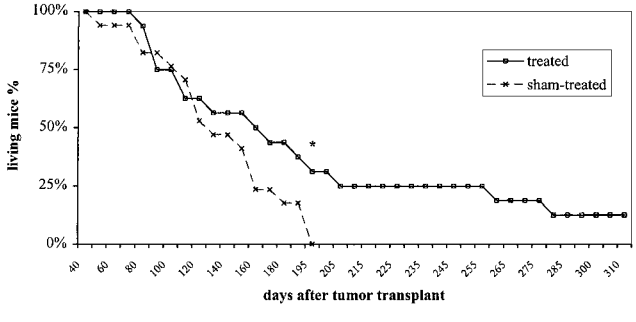

Fig. 2. Animal survival study. The curve reports the number of mice still alive on different days. Data refer to 16 treated and 17 shamtreated animals from day 1 to their natural death. (*$P < 0.05$ on the basis of Mantell-Cox test).

Tumor Growth Study

Given the increase in survival of the mice bearing WiDr tumor following the exposure to MF, we wanted to investigate the effect of the treatment on the tumor growth. Exposure to MF started when xenografts reached a mean tumor volume of 500 ± 200 mm^3 (V_b). After 4 weeks of treatment, MF exposed mice showed a tumor mass (V_e) significantly smaller (1200 ± 600 mm^3) than that of sham treated mice (2000 ± 900 mm^3), indicating a tumor growth inhibition of

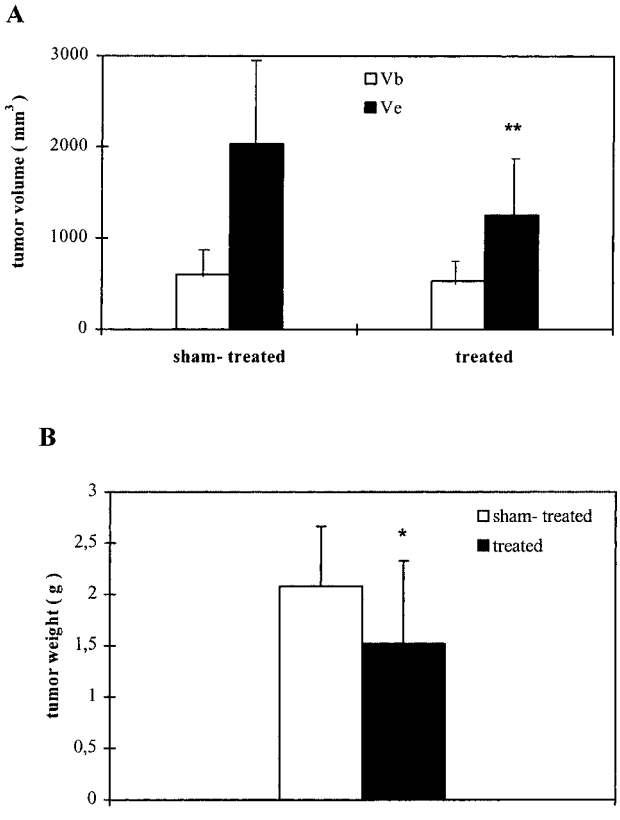

Fig. 3. Effect of MF on tumor growth inhibition and tumor weight. **A:** Tumor mass volume (in mm^3) at the beginning of treatment (V_b) and extracted at autopsy (V_e) after the 20th treatment. **B:** Weight (in g) of tumor mass at autopsy after the 20th treatment. Values are means and SDs considering all animals (N = 12 mice FM exposed, N = 9 mice shamexposed). (*$P < 0.05$, **$P < 0.01$ on the basis of Student's test).

40% (Fig. 3A). A confirmation of the tumor response to the treatment was given by the actual reduction (29%) of the tumor weight at necropsy (sham-exposed = 2.1 ± 0.6 g, MF exposed = 1.5 ± 0.8 g) (Fig. 3B). No difference in tumor growth was observed between sham treated mice and control mice housed under standard conditions without any manipulation (data not shown).

Under light microscopy, the histopathological examination of the tumor masses in most of the treated and untreated cases showed a moderately differentiated adenocarcinoma (Fig. 4). At microscopical analysis, necrosis, flogosis and fibrosis did not demonstrate significant differences between exposed and sham exposed mice. On the contrary, differences were detected as regards the number of mitoses (Fig. 4) the immunophenotypical expression of p53, and the number of apoptotic cells (Fig. 5). The analysis of

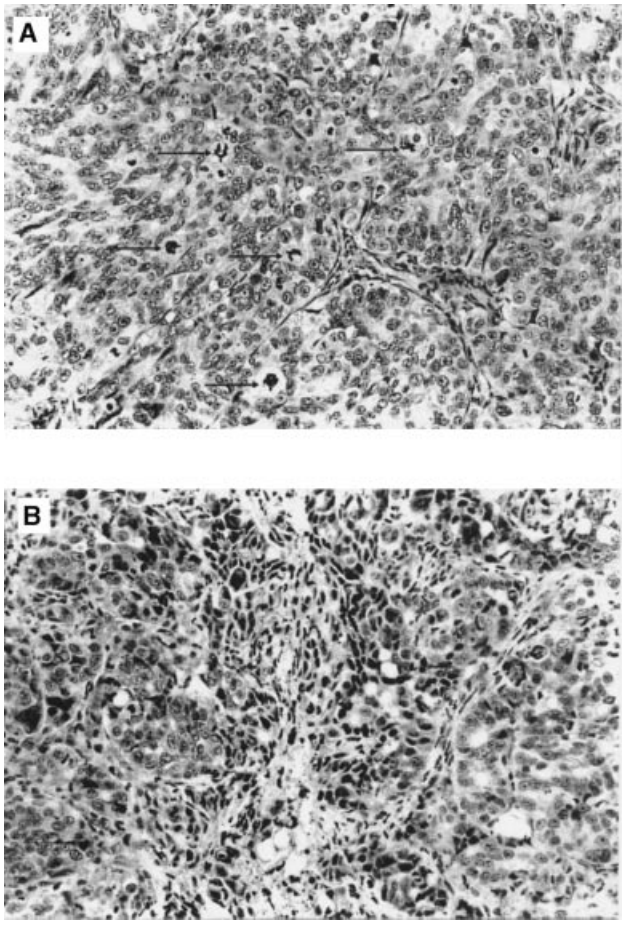

Fig. 4. Histopathological pictures of experimental tumor showing a moderately differentiated adenocarcinoma. In a sham exposed case (**A**), numerous mitoses (arrows) are present, while an MF exposed case (**B**) shows a lower number of mitoses and a great number of apoptotic figures, identified by dark "angular" nuclei. Magnification A,B ×200.

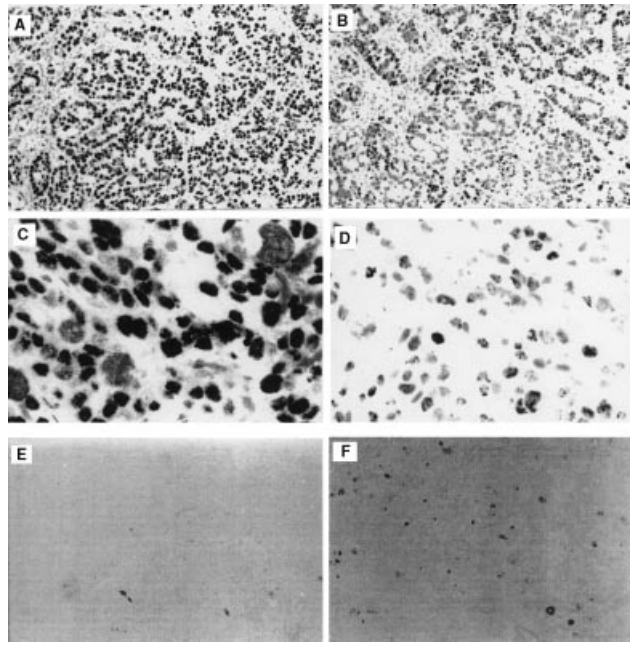

Fig. 5. Light microscopy of experimental tumors showing p53 expression by immunohistochemistry and apoptosis in situ by TUNEL. **A**,**C:** Intense p53 protein expression in the majority of neoplastic nuclei in sham exposed animals. **B**,**D:** Fewer positive nuclei, to a lower degree, are stained in experimental tumors of MF exposed animals by the same antibody. **E:** Rare apoptotic bodies (identified by dark "angular" nuclei) are shown in the sham-exposed animals, while (**F**) in the MF exposed ones apoptosis in situ is much more evident. Magnification; A,B × 100; C,D ×400; E,F ×100.

the immunohistochemical stain and DNA labeling for the detection of apoptosis shows that p53 expression (Fig. 6, panel A) significantly decreases (58%) and apoptotic index (Fig. 5, panel B) significantly increases (98%) in exposed animals. In addition the mitotic index and the Mib1 labeling index reported significantly decreased values corresponding to a 47 and 15% reduction, respectively.

At ultrastructural analysis (Fig. 7) in the exposed animals, a high number of ''dark'' cells, rich in highly electrondense cytoplasmic matrix were observed. They contained vacuoles filled with lipidic material. A ''rarefaction'' of perinuclear areas was seen in some cases and swollen mitochondria were present in high numbers. The basal membrane was often disrupted and a high number of apoptotic figures was found.

Safety and Toxicology Assessment

No morphological differences between exposed and sham exposed mice were seen at the histopathological analysis of any examined organ. However, less diffuse hepatocellular hypertrophy and a lower degree of splenic hematopoiesis, including the number of megakaryocytes, were seen in the treated animals than

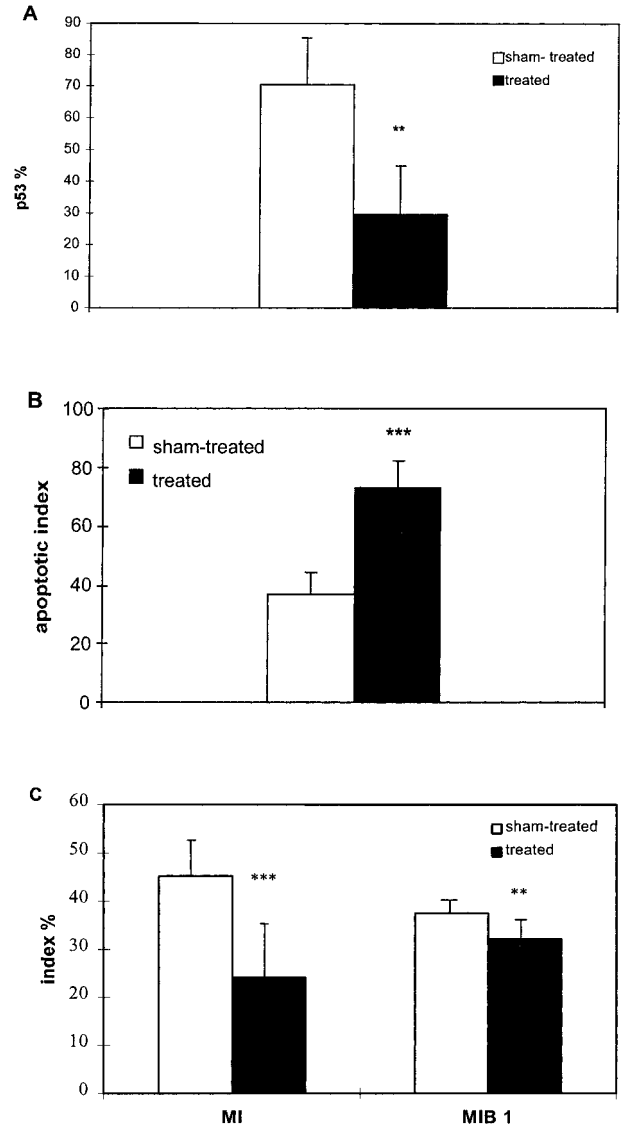

Fig. 6. Immunohistochemical analyses and mitotic index on tumor mass section. **A:** Labeling index for p53 antibody. **B:** Apoptotic index corresponding to the number of apoptotic cells found in 5,000 cells/mouse. **C:** Mitotic index (MI) and labeling index for Mib1 antibody. Values are means and SDs considering all animals for each experimental group (12 mice FM exposed and 9 mice sham exposed). ($^{**}P < 0.01, ^{***}P < 0.001$ on the basis of Student's test).

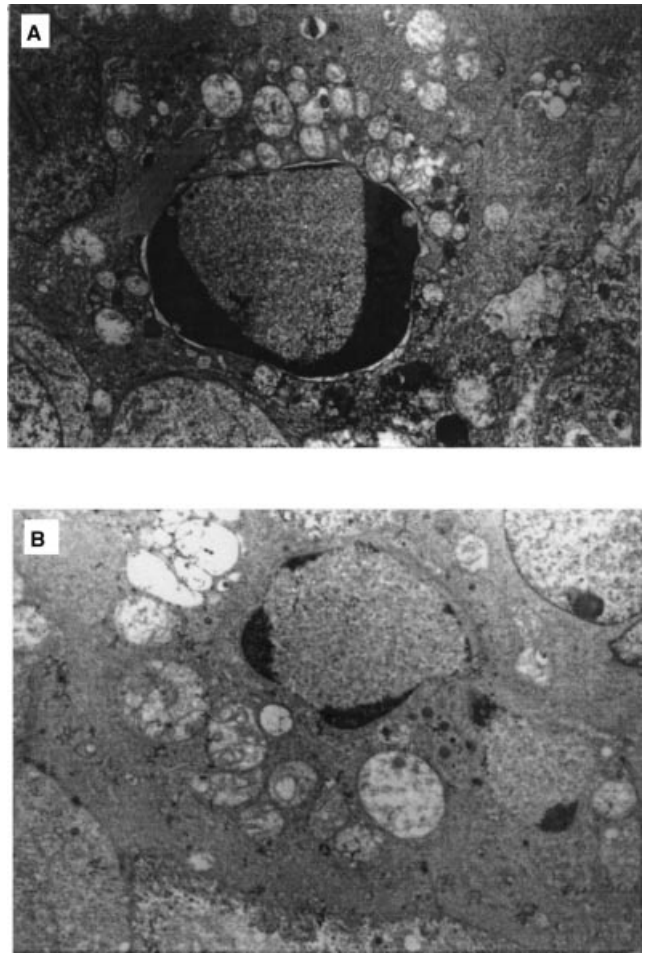

Fig. 7. **A,B:** Electron microscopy of MF exposed tumors. Apoptotic figures in different phases among neoplastic epithelial cells. Presence of vacuoles filled with lipidic-like material and numerous, swollen mitochondria in the cytoplasms of neoplastic cells. Magnification, ×450.

in the sham ones. The values of blood parameters reported in Table 2 demonstrated no significant changes in the exposed mice, with the exception of a significant decrease of the alanine aminotransferase levels that confirms the observed histological absence of hepatic necrosis in exposed mice. The lower hepatocellular hypertrophy and the decrease in alanine aminotransferase in exposed mice could be related with the reduced size of the tumor masses seen in exposed animals compared to the sham exposed since large tumor masses and the associated long-lasting necrosis are considered to cause metabolic overloading of the liver.

DISCUSSION

The present study shows that exposure to MF increases the survival and inhibits tumor growth of mice bearing a subcutaneous WiDr human colon adenocarcinoma. In addition, significant variation (by about 50%) in mitotic index (decrease), apoptosis (increase), and immunoreactive p53 protein (decrease) were observed in tumor tissues analyzed at the end of the exposure time. These results confirm the anticancer activity of MF with intensity of more than 1 mT, we previous reported on tumor growth inhibition using the same animal model [Tofani et al., 2001].

TABLE 2. Results of Blood Tests in All Animals of Experiment 2

Variable	Sham treated	Treated
Blood chemical constituent		
Urea nitrogen (mg/dl)	66.4 ± 27.9	80.9 ± 53.6
Creatinine (mg/dl)	0.2 ± 0.2	0.3 ± 0.4
Calcium (mg/dl)	10.4 ± 1.2	11.2 ± 0.9
Phosphorous (mg/dl)	7 ± 1.8	6.1 ± 0.8
Uric acid (mg/dl)	3.3 ± 1.2	4.0 ± 1.5
Total bilirubine (mg/dl)	1.3 ± 0.6	1.6 ± 0.8
Gamma glutamyl transferase (U/L)	2.4 ± 1.3	5 ± 3.6
Alkaline phosphatase (U/L)	16.9 ± 8.8	19.6 ± 14
Aspartate amino transferase (U/L)	666.17 ± 257.6	628.4 ± 277.3
Alanine aminotransferase (U/L)	241.5 ± 112.8	146.8 ± 65*
Hematoclinical parameter[a]		
Hemoglobin (g/dl)	14.2 ± 0.7	13.6 ± 1.1
Hematocrit (%)	42 ± 2.2	39.9 ± 2.6
Red blood cell count (cells$\times 10^6$/μl)	8.4 ± 0.3	8.1 ± 0.5
MCV (μm^3)	50.3 ± 1.2	49.3 ± 0.5
MCH (pg)	16.9 ± 0.4	16.9 ± 0.7
MCHC (g/dl)	33.7 ± 0.6	34.2 ± 1.5
White cell count (cells$\times 10^3$μl)	4.6 ± 1.3	4.8 ± 2.4
Platelet count (cells$\times 10^3$μl)	696 ± 164.4	621.8 ± 152.4
MPV (μm^3)	8.7 ± 2.7	11 ± 5.8

Values are mean and SDs considering all animals for each experimental group (N = 12 mice MF exposed; N = 9 mice sham exposed). (*$P < 0.05$ on the basis of Student's test).

The observed tumor growth inhibition appears to be associated with morphological changes only in transformed cells. No morphological changes in renewing (i.e., bone marrow cells), slowly proliferating (i.e., hepatocytes) and static (i.e., neurons) normal cells were observed. In addition, no significant differences in the number and morphology of blood corpuscular elements, emunctory function of liver and kidney, and bone metabolism were detected, between the exposed and the sham exposed animals. The lack of adverse responses in normal cells and tissues suggests that the safety of this treatment may be related to its ability to interfere preferentially selectively with transformed cells.

It is well known that a loss of p53 functional status, either due to lack of gene expression or overexpression of a mutant form, leads to genomic instability and cancer [Sherr, 1996]. The most frequently encountered mutations of p53 reduce its thermodynamic stability determining the loss of the DNA binding conformation indispensable to the transcription regulation and tumor suppressor activity [Bullock et al., 1997]. Pharmacological rescue of mutant p53 conformation and function have been also reported [Foster et al., 1999]. Others demonstrated that metal ions, such as Zn^{2+}, play a regulatory role in the control of p53 folding and DNA binding activity [Meplan et al., 2000]. Specific DNA binding is influenced by redox regulation of p53, and binding of metal ions may directly affect p53 redox potential, either at the zinc binding cysteine residues or at other cysteine residue on the protein surface [Wu et al., 1999].

Thus, based on these data, we suggest that the observed decrease of p53 immunostaining after MF exposure, together with the increased apoptotic index and the slower growth of experimental tumors, could be explained by a rescue of wild type p53. This phenomenon could be related to the effects of MF exposure redox chemistry connected to metal ions. Further studies will be necessary to elucidate the biomolecular pathways at the basis of our results, including the use of transformed cell lines nonexpressing mutated p53.

This study shows that MF exposure caused a moderate response with only 40% tumor growth inhibition. This low efficacy represents one limitation for the development of this therapy. However, it is worth noting that, MF exposure affects early tumor growth (exposure started at day 1 of tumor transplant, see Fig. 2) as well as advanced tumors (Fig. 3). These findings, together with the apparent lack of toxic and adverse side effects, are in favour of a prolonged period of exposure to MF and a combination with conventional therapies, such as cytotoxic agents. Previous works have addressed the combination of conventional antitumor therapies and electromagnetic fields [Cadossi et al., 1991; Pasquinelli et al., 1993; Chakkalakal et al., 1999]. Once further experimental

information on the biomolecular-biophysical mechanism is available, the possibility of changing treatment characteristics (i.e., intensity) and treatment timing may lead to higher anti-cancer efficacy.

In conclusion, MF treatment is a novel approach that might contribute to cancer research and therapy, and as such deserves further investigation.

ACKNOWLEDGMENTS

The authors express their gratitude to Raffaella Giavazzi of Mario Negri Institute for Pharmacological Research for her valuable advice and critical review of the manuscript. Gratitude is also expressed to Lorenzo Silengo of Turin University for his numerous helpful discussions and advice.

REFERENCES

Basset CA, Mitchell SN, Gaston SR. 1982. Pulsing electromagnetic field treatment in ununited fractures and failed arthrodeses. JAMA 247(5):623–628.

Bullock AN, Henckel J, DeDecker BS, Johnson CM, Nikolova PV, Proctor MR, Lane DP, Fersht AR. 1997. Thermodynamic stability of wild-type and mutant p53 core domain. Proc Natl Acad Sci USA 94:14338–14342.

Cadossi R, Zucchini P, Emilia G, Franceschi C, Cossarizza A, Santantonio M, Mandolini G, Torelli G. 1991. Effect of low frequency low energy pulsing electromagnetic fields on mice injected with cyclophosphamide. Exp Hematol 19(3):196–201.

Chakkalakal DA, Mollner TJ, Bogard MR, Fritz ED, Novak JR, McGuire MH. 1999. Magnetic field induced inhibition of human osteosarcoma cells treated with adriamycin. Cancer Biochem Biophys 17(1-2):89–98.

de Seze R, Tuffet S, Moreau JM, Veyret B. 2000. Effects of 100 mT time varying magnetic fields on the growth of tumors in mice. Bioelectromagnetics 21:107–111.

Dibirdik I, Kristupaitis D, Kurosaki T, Tuel-Ahlgren L, Chu A, Pond D, Tuong D, Luben R, Uckun FM. 1998. Stimulation of Src family protein–tyrosine kinases as a proximal and mandatory step for SYK kinase-dependent phospholipase Cgamma2 activation in lymphoma B cells exposed to low energy electromagnetic fields. J Biol Chem 273:4035–4039.

Foster BA, Coffey HA, Morin MJ, Rastinejad F. 1999. Pharmacological rescue of mutant p53 conformation and function. Science 286:2507–2510.

Gray JR, Frith CH, Parker JD. 2000. In vivo enhancement of chemotherapy with static electronic or magnetic fields. Bioelectromagnetics 21:575–583.

Hendee WR, Boteler JC. 1994. The question of health effects from exposure to electromagnetic fields. Health Phys 66:127–136.

Hisamitsu T, Narita K, Kasahara T, Seto A, Yu Y, Asano K. 1997. Induction of apoptosis in human leukemic cells by magnetic fields. Jpn J Physiol 47:307–310.

Koifman S. 1993. Electromagnetic fields: a cancer promoter? Med Hypothesis 41:23–27.

Kristupaitis D, Dibirdik I, Vassilev A, Mahajan S, Kurosaki T, Chu A, Tuel-Ahlgren L, Tuong D, Pond D, Luben R, Uckun FM. 1998. Electromagnetic field-induced stimulation of Bruton's tyrosine kinase. J Biol Chem 273:12397–12401.

Meplan C, Richard MJ, Hainaut P. 2000. Metalloregulation of the tumor suppressor protein p53: zinc mediates the renaturation of p53 after exposure to metal chelators in vitro and in intact cells. Oncogene 19:5227–5236.

NIEHS, National Institute of Environmental Health Sciences. 1999. NIEHS Report on health effects from exposure to power-line frequency electric and magnetic fields, NIH Publication No 99-4493.

NRC, National Research Council. 1996. Committee on the Possible Effects of Electromagnetic Fields on Biologic Systems. Possible Health Effects of Exposure to Residential Electric and Magnetic Fields. Washington, DC: National Academy Press.

Pasquinelli P, Petrini M, Mattii L, Galimberti S, Saviozzi M, Malvaldi G. 1993. Biological effects of PEMF (pulsing electromagnetic field): an attempt to modify cell resistance to anticancer agents. J Environ Pathol Toxicol Oncol 12(4):193–197.

Sherr CJ 1996. Cancer Cell cycles. Science 274:1672–1677.

Simko M, Kriehuber R, Weiss DG, Luben RA. 1998. Effects of 50 Hz EMF exposure on micronucleus formation and apoptosis in transformed and nontransformed human cell lines. Bioelectromagnetics 19:85–91.

Tofani S. 1999. Physics may help chemistry to improve medicine: a possible mechanism for anticancer activity of static and ELF magnetic fields. Phys Med 15:291–294.

Tofani S, Barone D, Cintorino M, de Santi MM, Ferrara A, Orlassino R, Ossola P, Peroglio F, Rolfo K, Ronchetto F. 2001. Static and ELF magnetic fields induce tumor growth inhibition and apoptosis, Bioelectromagnetics 22:419–428.

Wu HH, Sherman M, Yuan YC, Momand J. 1999. Direct redox modulation of p53 protein: potential sources of redox control and potential outcomes. Gene Ther Mol Biol 4:119–132.